Chapter 5

NONLINEAR ELECTRICAL CONDUCTIVITY OF METAL NANOCONTACTS IN THE BALLISTIC REGIME

5.1 Abstract

In this PhD project we devoted special efforts to the analysis of the quasiparticles relaxation kinetics of NCs in the ballistic regime for the whole range of excitation energies. The electron-phonon interaction part of the PC spectra ($eV<hf_D$), caused by the spontaneous phonon generation, changes very little for high frequencies, while the background part ($eV>hf_D$), brought about by the reabsorption of non-equilibrium phonons, transforms significantly under HF irradiation.

The interesting phenomenon of the background signal which decreases as the frequency of the radiation increases, discovered earlier by different authors [1, 2], was investigated in details. As will be illustrated below, we could calculate the characteristic frequency for phonon-electron interaction in Cu, and establish the classical and quantum detection frequency ranges as well as the characteristic frequency for the transition to a bolometric response.

Improved resolution of PCS at high frequencies $f>f_T$, $f_{ph\text{-}e}$, (where f_T is the thermal relaxation frequency of the NC, and the $f_{ph\text{-}e}$ is the frequency of non-equilibrium phonon on electron

relaxation) due to reduced reabsorption of non-equilibrium phonons was proved.

Spectra with negative sign of second derivative $d^2V/dI^2<0$ (inversed spectra) for Sb, a semi-metal characterised by a low carrier concentration and a low Fermi energy, and their frequency dispersion were studied.

As for the NCs in the thermal regime, we performed systematic studies of the non-linear properties of ballistic NCs of Cu in the wide frequency range (10^3-$4{,}78\cdot10^{14}$ Hz), and observed the transition from classical to quantum detection regime.

From the frequency dependence of the background reduction coefficient we could deduce the frequency for non-equilibrium phonon relaxation in Cu - an important parameter for the phonon-electron kinetics.

The investigation of the bolometric response when irradiating with visible light established the importance of direct laser heating of the lateral surface of the NC.

The experimental results concerning the response to irradiation in the optical frequency range allowed to establish a special type of PCS, namely Laser Thermal Point-contact Spectroscopy, characterized by a better resolution of spectral singularities.

5.2 Experimental Results and Theoretical Analysis of the Relaxation Kinetics for Cu Nanocontacts in the Ballistic Regime

Phonon and PC spectra of Cu have been studied extensively [1-4]. In the present work, the investigated NCs were of " pin-to-plate" geometry with contact resistances in the range of 0,5-7 Ohm. In each measurement cycle, the PC spectrum of the contact and a series of response signals at HF irradiation were registered. At the end of each cycle, the acoustic frequency (~1 kHz)

spectrum was compared with the initial one to verify the stability of the contact. All spectra were normalised to the maximum intensity of Transverse-phonons (T-phonons) peak, as to neglect the background at this energy.

All NCs reported in this chapter were in the ballistic current regime as proven by the high intensity of the spectral singularities, by the relatively low background level of the response to HF irradiation and also by the calculated characteristic contact parameters. The EPI part of the spectra ($eV<hf_D$) due to spontaneous phonon generation changes very little for HF (Fig. 5.1), while the background part ($eV>hf_D$) due to reabsorption of non-equilibrium phonons varies significantly. The reduction of the background in the HF spectra evidences a new spectral singularity that occurs at a combination of transverse and longitudinal phonon energies, $hf_t + hf_l$, shown in Fig. 5.1 with an arrow. The results for the Cu NCs presented in Figs. 5.1 and 5.2 were obtained earlier by different authors [1, 2]; with the present work these results were completely confirmed. Extensive studies of these phenomena permitted us a detailed analysis of the relaxation kinetics for Cu NCs [5, 14, 19, 20].

A gradual decrease of the background signal at MW frequencies was observed for the bias values $eV>hf_D$ up to 100 meV (Fig. 5.1). Such a behaviour is not predicted by theory. Another unexpected experimental result was the saturation of the background with increasing frequency of the impinging radiation; in fact, (2.23) predicts that the background signal decreases monotonously to zero as the frequency rises.

The response signal, $V_{d,}$ for all NCs was measured at minimal power levels at mW range. With increasing power a linear increase of the response signal (Fig. 5.2) was observed [2, 5] which confirms that the normalisation of the response values to the maximum of the T-phonons peak is correct.

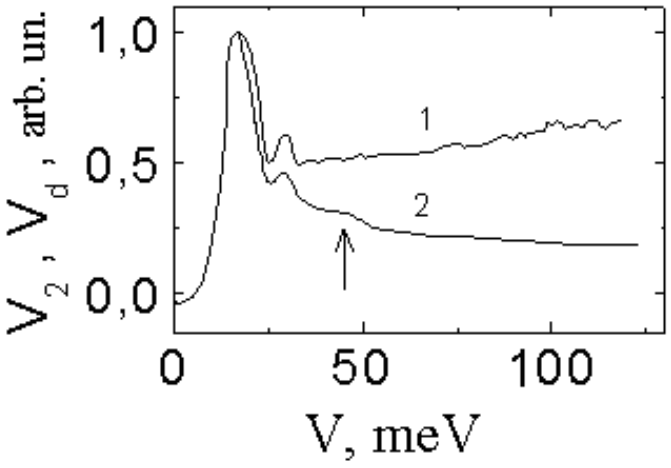

Fig. 5.1 Point-contact spectra of Cu measured [1, 2] at acoustic frequency (~1 kHz) (1) and at microwave frequency (80 MHz) (2).

In the following we focus on the nature of residual background in the PC spectra collected at HFs. The deviation of the experimental results from the theoretically predicted monotonous dependence ($\eta \sim 1/f^2$) can be explained as follows. The measurement of the video-detection signal for a given transport current is performed by registrating the voltage difference V_d on the NC under irradiation and in the dark (3.4). When the IVC does not depend on frequency, the V_d value is determined by the rectification of the alternating HF current on the IVC non-linearities, and for small modulation amplitudes the signal V_d is proportional to the second derivative of the IVC. In the case of HF ($f > f_{ph\text{-}e}$), the IVC are modified because of a different contribution of the phonon reabsorption to electron scattering. The V_d value will not be only due to HF rectification, but also

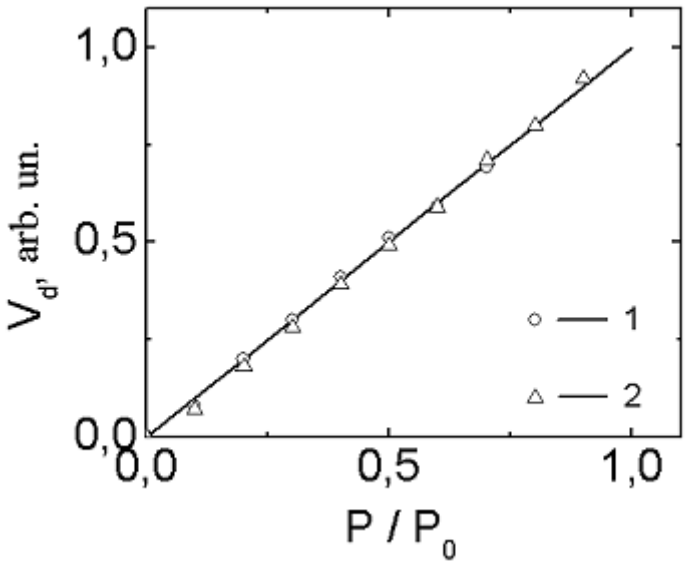

Fig. 5.2 The dependence of response signal on the power (at mW level) of the high frequency radiation for Cu nanocontacts [2], at 17 mV (1) and 60 mV (2) bias voltage.

depends on the modification of the IVC under irradiation. This additional contribution is due to the excessive amount of non-equilibrium phonons generated in the NC by the HF current, at bias $eV>hf_D$. It can be referred to as a bolometric contribution, *i.e.* as modification of the NC resistance with HF irradiation. The higher the irradiation frequency, as smaller the part of non-equilibrium phonons that follows the HF current because of the phonon relaxation inertia.

The NC temperature increases under HF irradiation only in the thermal regime (Chapter 4). The experiments prove and theory confirms that a frequency increase in the range $f>f_T$ (where $f_T \approx sl_i/d^2$ is the thermal relaxation frequency of NC) brings about a non-linear relation between bias and contact temperature. For the contacts in the ballistic regime, the stationary part of the NC temperature is referred to as an effective temperature of the

phonon subsystem, and is higher than the ambient (Helium bath) temperature. The electron subsystem continues to have the ambient temperature.

As theoretical works show, when the elastic mean free paths of phonons and electrons are approximately the same, the thermal relaxation frequency (f_T) is similar to the frequency of non-homogeneous escape of phonons from the NC, and both these frequencies are almost equal to the frequency of phonon-electron interactions $f_{ph\text{-}e}$. As the radiation frequency increases, the rectification part of response signal V_d decreases, while the bolometric contribution grows and finally dominates the response signal. The amplitude of the bolometric component is proportional to the contact current and to the resistance change under irradiation; it grows monotonously with the current. This consideration clarifies the background signal behaviour. At high enough frequencies ($f>f_{ph\text{-}e}$) and small bias ($eV<hf_D$), the video response signal is determined mainly by the rectified HF current. With increasing bias, this part tends to zero, while the bolometric part (proportional to the first derivative of IVC) intensifies. A similar behaviour was described before (Chapter 4) for contacts in thermal regime exposed to alternating electromagnetic fields of frequencies $f>f_T$.

Another characteristic feature of the HF spectra is the intensity decrease of the response at bias voltages in the range $eV>hf_D$. Fig. 5.1 shows a saturation for bias voltages around 100 mV [1, 2], which can be explained with an intermediate phase of phonon gas thermalization occurring through phonon-phonon collisions. The probability of such interactions is of one order of magnitude higher than that of phonon-electron interactions. The effective phonons temperature (2.20), i.e. the number of non-equilibrium phonons increases with bias voltage. The frequency of this process is limited by the thermal capacity of the phonon subsystem. The thermal capacity grows with temperature,

increasing the thermalization time and hence the inertia of the phonon system. The saturation of thermal capacity occurs at the temperatures higher than the Debye temperature $T_{eff}>\Theta_D$, which corresponds to $eV=4k_B\Theta_D=110{,}3$ meV for Cu as seen experimentally in Fig. 5.1.

As noted before, the HF measurements for Cu give evidence for a spectral singularity at $eV\sim45$ meV, absent in the low frequency measurement. One of the reasons for the worse resolution of conventional low frequency Point Contact Spectroscopy is heating of the NC by the transport current. At frequencies $f>f_T$, $f_{ph\text{-}e}$, reabsorption of non-equilibrium phonons and thermal effects are reduced, and hence the resolution of HF spectroscopy is improved. This phenomenon does not influence the spontaneous generation of phonons by non-equilibrium electrons, as soon the operational frequencies $f<<f_{e\text{-}ph}$.

Due to the improved resolution and the fact that additional information that can be retrieved from HF measurements, this method is considered as a new kind of PCS and called High Frequency Point-Contact Spectroscopy.

5.3 Relaxation Kinetics of Non-Equilibrium Phonons in Sb Nanocontacts

The investigation of semi-metallic NC such as Sb, characterised by a low carrier concentration and a low Fermi energy (comparable with phonon energies) permits to discover new effects, for instance trajectory effects for ballistic contacts (when the Larmor orbital radius for electrons is comparable with the NC diameter), and quantum interference effects related to localised electronic states [6, 7]. However, other authors encountered difficulties when trying to explain the background part of the spectra, which is usually attributed to reabsorption processes of non-equilibrium phonons. The nature of the background signal

for Sb was not clear up to now. We performed HF PCS experiments with Sb [8, 9], and explained them based on the big difference in relaxation frequencies for electrons and phonons in metals (~10^3).

The spectra obtained experimentally agree well with the ones known from literature [6, 7] for the same orientation of NC axis relative to crystallographic axis of Sb. The PC spectra of the EPI present (see lines 1 in Fig. 5.3-5.5) a singularity at an energy eV≈2 meV, which can be attributed to intravalley electron scattering processes, as well as two main peaks due to intervalley processes involving acoustic (eV≈7,3 meV) and optical (eV≈17,5 meV) phonon modes. The good quality of the contacts is indicated by the high intensity of the main peaks, as well as by

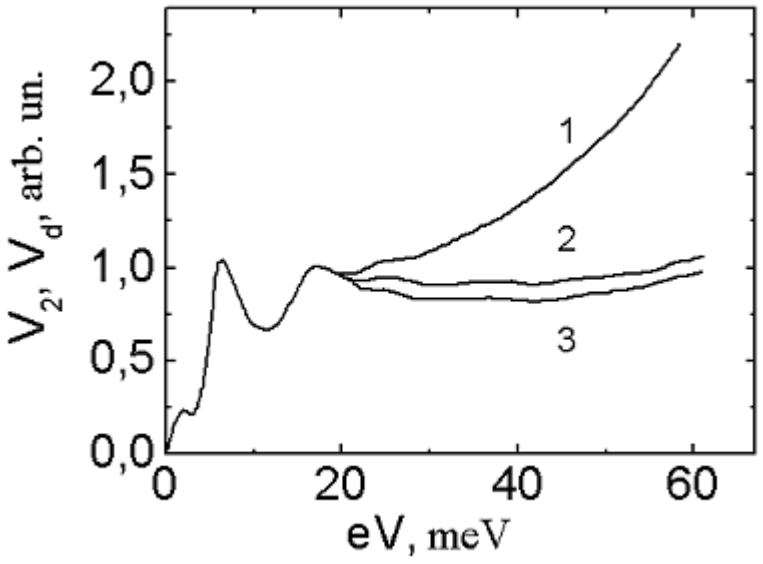

Fig. 5.3 Point-contact spectra of Sb, measured at acoustic frequency (~1 kHz) (1) and in the high frequency range: at 0,6 GHz (2) and at 70 GHz (3). Contact resistance R_0=0,74 Ohm.

the presence of singularities at energies which are a multiple or a sum of of the fundamental ones and hence associated with multi-phonon generation processes. At higher bias $eV \approx 175$ eV a big maximum of thermal nature can be seen; this phenomena was analysed before (section 4.2).

It has been reported elsewhere [6, 7] that for dirty Sb NCs present EPI spectra of a negative sign of second derivative $d^2V/dI^2<0$ (inverse spectra). The same is true or for contacts obtained through multiple contacting of electrodes. The latter procedure implies creating a considerable amount of deformation (cold-work hardening) of the Sb crystal structure. According to [6], the elastic mean free path l_i in these crystals may be of the order of 10 nm, which is comparable with de Broglie wavelength $\lambda_F=2\pi\hbar/p_F$ (p_F is the Fermi momentum) of carriers in Sb due to the small value of p_F ($\varepsilon_F \sim 90$ meV). The condition $l_i \approx \lambda_F$ brings about the possibility of spatial localization of electron states. The scattering of non-equilibrium electrons by phonons in a NC causes a phase lag between electron wave functions, i.e., it violates the quantum localization and hence leads to an increase in the conductivity of the contact ($d^2V/dI^2<0$ with DC bias increasing) and so, to the inverse spectra.

The theory of quantum interference effects in the electrical conductivity of NCs was developed in [10]. Figure 5.4 shows the inverse EPI spectrum obtained after contacting the electrodes repeatedly. The main characteristic features of this spectrum are in good agreement with the data of [6, 7]. As can be seen in Fig. 5.4, the background of the inverse spectrum is negative.

The emergence of a background in PC spectra is associated with the reabsorption of non-equilibrium phonons by the electron flow. For large bias voltages across a contact, the number of non-equilibrium phonons increases with voltage, and so does the number of scattering events of the electrons. In other words, the contact resistance (the first derivative) also increases, and hence

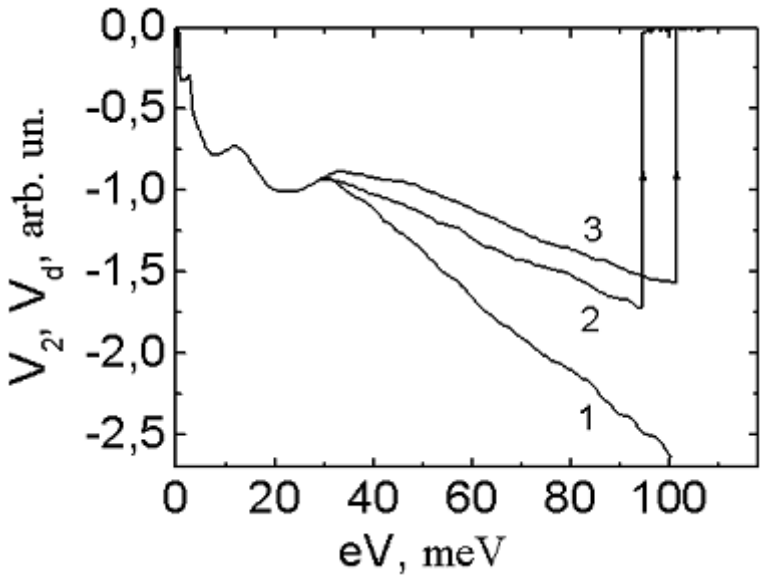

Fig. 5.4 Inverse point-contact spectra of Sb (1) and video response at frequencies 0,59 GHz (2) and 70 GHz (3). Contact resistance R_0=2,05 Ohm.

the second derivative will have a positive nonzero value in this energy range. In the presence of quantum phase-coherent localization effects, the above-mentioned processes violate the localization in the NC, the contact resistance decreases with increasing eV, and the second derivative will be negative.

When the contact is exposed to radiation in the MW wave range, the processes of emission and reabsorption of non-equilibrium phonons by electrons are separated in time due to a considerable difference between the characteristic relaxation times of the electron and phonon subsystems of the metal. This allows us to establish where the background in the PC spectra originates from and to determine the characteristic phonon relaxation times. The phonon-electron relaxation frequency for Debye phonons in Sb can be estimated from (2.22). Using the

values s=3,4·10^5 cm/s for the speed of sound, v_F = 0,7·10^8 cm/s for the Fermi velocity, Θ_D=210 K for the Debye temperature for Sb, and λ=0,09 for the EPI constant obtained from NC studies [6], we obtain $f_{ph\text{-}e}$=1,8 GHz. Taking this value of the characteristic phonon relaxation frequency into account, we measured the microwave PC spectra for exposure to electromagnetic radiation with frequency in the interval 0,1-80 GHz.

The microwave PC spectra of Sb are shown in figures. 5.3 and 5.4 (lines 2,3) for two different frequencies of the impinging radiation. For inverse MW spectra, the radiation was specially screened by an attenuator at the end of recording in order to control the negative sign and its zero level. Fig. 5.5 shows the analogous result for another NC in which a partial spatial

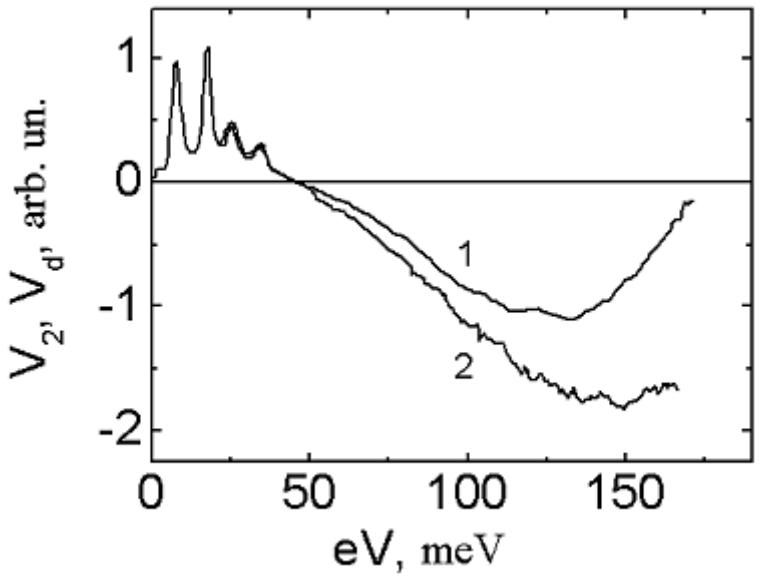

Fig. 5.5 Point-contact spectra of Sb at acoustic frequency (~1 kHz) (1) and at 80 GHz (2). Contact resistance R_0=3,57 Ohm.

localization of electron states appears to take place. For all measurements, the intensity of the MW radiation was chosen in such a way that amplitudes of main EPI peaks at low and high frequencies coincide. Such a normalization of signals correlates the difference between the coefficients of coupling for the NC and external MW field and allows a direct measurement of the frequency dispersion of the response signal.

From the results presented in Figs. 5.3-5.5 follows that for large bias voltages across the contacts, one observes a considerable decrease in video response signal in the background region even for frequencies of the impinging radiation of a few hundred MHz. A further increase in frequency by two orders of magnitude (up to 80 GHz) causes only a slight change. The background signal is found to increase with DC bias voltage across the contact. This increase in background may be observed even in the inverse spectrum region as shown in Fig. 5.5. As noted before (section 4.2), such a behaviour is determined by the contribution of thermal effects.

We shall now analyze the behaviour of the background signal for various radiation frequencies in the energy interval 30-60 meV in the immediate vicinity of the EPI spectrum. It follows from data presented in Figs. 5.3-5.5 that the maximum variation in background amplitude occurs in the acoustic frequency interval up to ~0,6 GHz, and can be attributed to the emergence of thermal effects (see above). Moreover, the frequency dispersion of the background in the interval 0,6-80 GHz is quite insignificant, and a high level of residual background signal is observed even when the measurements are carried out at the limiting frequency of 80 GHz.

The weak dispersion of background in the interval of frequencies close to the characteristic phonon-electron collision frequency in Sb $f_{ph\text{-}e}$~2 GHz points to a low intensity of reabsorption processes of non-equilibrium phonons that can leave the NC region without being scattered by electrons.

In view of this weak reabsorption of non-equilibrium phonons in Sb contacts, we can't attribute the high level of residual background for f~80 GHz to the bolometric effect (i.e., to the presence of non-equilibrium phonons in NC, as it was done before in section 5.2, for Cu NCs). In all probability, the residual background is due to rapid electron-phonon scattering processes with a high characteristic frequency $f_{e\text{-}ph}\sim\lambda f_D\sim10^{13}$ Hz. Therefore we conclude from Fig.s 5.3-5.5 that due to the energy dependence of the electron-phonon relaxation length, Sb NCs undergo a transition from the ballistic ($l_i,\ l_\varepsilon>>d$) or diffusive ($(l_i\ l_\varepsilon)^{1/2}>d$) regime to the thermal one ($l_\varepsilon\ l_i,<<d$). According to the theory of PCS in the dirty limit [11], the intensity of multi-phonon generation processes increases due to energy relaxation of the electrons in the NC. The presence of a background contribution from electron relaxation apparently necessitates the introduction of a phenomenological correction [6], which increases linearly with bias voltage.

All the above considerations concerning possible reasons behind the observation of frequency dispersion of the background signal are also applicable to contacts with localized electron states possessing inverse PC spectra. We can neglect the direct influence of the electromagnetic field on the phase lag between electron wave functions in the NC [12, 13] for energies higher than the Debye energy because of the small characteristic times $\tau_\varphi\sim\tau_{e\text{-}ph}\sim10^{-13}$ s in this energy region. The situation becomes a little more complicated for the contact presented in Fig. 5.5. In spite of a positive EPI spectrum of the NC, the background becomes negative upon increasing the voltage, and then, at even higher values of eV tends to come back to positive values characteristic for a thermal anomaly of the IVC. Such behaviour of the second IVC derivative can be explained by assuming that a fraction of conduction electrons in the NC is localized in space in some part of the contact volume. PC spectral studies for Sb show

that the response of NCs is described correctly by the "T-model" [6] in which impurities are assumed to be concentrated in a narrow layer of thickness $T<d$ at the surface of the contacting electrodes, while the entire remaining NC volume is assumed to be clean. With an increase in the excess energy of the electrons, the EPI overcomes the localization of states in the impurity interlayer, and the resistance begins to decrease ($d^2V/dI^2<0$). However, the NC changes over into a thermal regime upon a further increase in voltage, and thereafter its resistance increases again. The behaviour of the second IVC derivative at HF (line 2 in Fig. 5.5) is determined by the competition between several relaxation mechanisms with different characteristic times ($\tau_{e\text{-}ph}$ at low energies, τ_φ and $\tau_{ph\text{-}e}$ at intermediate energies, τ_T at high energies) and is in good agreement with the proposed model.

5.4 Laser Thermal Point-Contact Spectroscopy of Metals

5.4.1 Experimental Results

In Chapter 4 we showed that the video response of NCs in the thermal regime contains spectral singularities, specific for low frequency spectra. Despite the large energy of optical photons ($\hbar\Omega$~2 eV for λ=0,63 μm), no broadening, characteristic for quantum detection process, of these singularities was observed. In this section we describe the studies of pure ballistic Cu NCs, performed to clarify the physical nature of video detection [5, 14].

To improve the coupling between electromagnetic radiation and NC, we used the "pin-to-plate" geometry. A spear-shaped electrode made of Cu wire of diameter 0,2 mm was sharpened to a diameter ~1 μm. The second electrode was a copper cylinder

with a polished end face or a Cu film of thickness 1,5 μm deposited on a 1,5 mm thick glass substrate. Both electrodes were brought together by a precision mechanism and the NCs were formed directly in liquid Helium.

Optical radiation was generated by a multimode He-Ne current wave laser of nearly 25 mW power at a wavelength λ=0,63 μm ($\Omega/2\pi$=4,75·10^{14} Hz, $\hbar\Omega$=1960 meV). The laser beam was focused through a quartz window in the cryostat walls by a lens to a spot diameter of 0,05 mm in the region of NC. The irradiation of the NC was performed in two different ways as sketched in Fig. 5.6: in the first case (a) the laser beam was directly focused on the NC; in second case (b) it was focused on the backside of the Cu film.

Direct laser beam irradiation of a contact.

For metal NCs, the region of relatively strong non-linearity of IVC associated with electron-phonon interaction extends to Debye energies and covers an interval up to tens of meV (~35 meV for Cu). The energy of a radiation quantum was $\hbar\omega$~2 eV. Hence, in accordance with (3.5), we can expect a monotonic increase in response upon an increase in constant bias voltage across the NC.

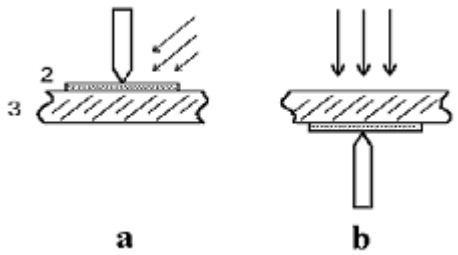

Fig. 5.6 Contact configuration and two methods of laser irradiation: 1 – spear; 2 – copper film; 3 – glass substrate.

The experimental result for the bias voltage dependence of the video response signal , $V_d(V)$, upon direct irradiation of a Cu contact with the laser beam and the corresponding low frequency spectrum are depicted Fig. 5.7 (a). As can be seen from the figure, the detected signal has well-defined spectral singularities whose shape and position coincide with the EPI spectrum of Cu with a slightly enhanced background level. The measurements were made at a NC temperature T=1,7 K in superfluid Helium. In normal Helium ($T>T_\lambda$), the amplitude of the response signal was found to be much larger. Replacement of a thin film electrode by a bulk Cu cylinder [1, 2] practically did not change the result and simply led to a manifold decrease in signal amplitude and to sharper spectral singularities due to a more perfect structure of the metal in a bulk electrode.

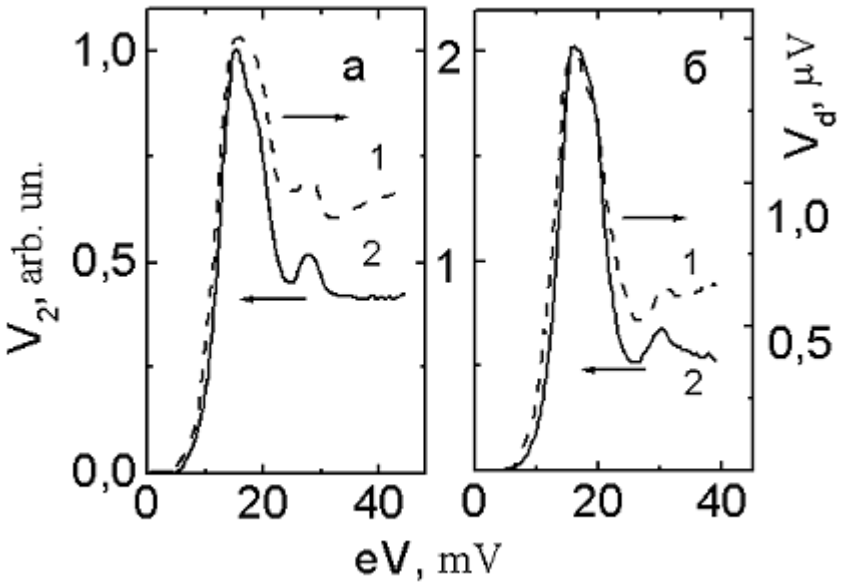

Fig. 5.7 Video response of a Cu contact (1) and its low frequency (~1 kHz) spectrum (2): upon direct irradiation (a) and upon heating (b) with laser beam.

Rotation of the polarization plane of the laser radiation led to a 20-30% variation in response signal amplitude, the maximum being observed when the projection of the electrical component of the external field was parallel to the spear.

The unusual shape of measured signal can be attributed to a broadening of the EPI spectral singularities under the action of the laser irradiation since the light frequency is comparable to the reciprocal time of flight of the electrons through the NC region. It follows from theory [15] that a dispersion of the conductivity should be observed under such conditions. For a contact whose characteristics are described in Fig. 5.7 (a), the reciprocal time of flight is $v_F/d \sim 2{,}2 \cdot 10^{14}$ Hz ($v_F = 1{,}57 \cdot 10^8$ cm/s is the Fermi velocity of electrons in Cu, and the contact diameter $d \sim 7{,}3$ nm is calculated from its resistance $R = 17$ Ohm). Such a broadening results in a smoothing of non-linear IVC regions under irradiation, and hence the difference in IVC measured in the modulation technique experiments assumes its highest value in these regions.

Another mechanism for the broadening of the EPI spectral singularities may be heating of the NC by laser radiation since heating broadens the Fermi edge. This explains the enhancement of the effect in He-I and for a film electrode which has a poorer heat removal from the hot spot as compared to bulk metal. The polarization dependence of the response intensity may be due to antenna properties of the spear or to a change in the absorption and reflection coefficients for different directions of the radiation polarization according to the Fresnel formula, and cannot serve as a proof of the non-thermal nature of the response.

Heating of a contact by a laser beam.

Focussing the laser on the backside of the Cu film (Fig. 5.6 (b)) corresponds to studying the processes associated with heating of the NC. The maximum amplitude of the recorded signal was

attained by scanning the surface of the film with a luminous spot. Under such experimental conditions, the role of the laser beam is reduced to generating a phonon flux on the NC.

Non-equilibrium electrons excited by an external electromagnetic field to energies $\hbar\Omega$~2 eV relax as a result of electron-phonon scattering and generate high-energy non-equilibrium phonons with low group velocities. As these phonons propagate through the film, equilibrium in the phonon subsystem is attained as a result of phonon-phonon scattering. In view of the large thickness and structural heterogeneity of the film, it can be assumed that the phonon distribution at the NC attains its equilibrium which is characterized by certain temperature value $T_0+\Delta T$ exceeding the thermostat (Helium bath) temperature T_0.

The experimentally measured dependence of thermal response on bias voltage is shown in Fig. 5.7 (b) along with the EPI spectrum of this NC. It can be seen that the results are practically the same as in Fig. 5.7 (a) for direct exposure to light. Measurements were carried out on a contact with resistance R=16 Ohm at a temperature T_0=2,8 K and a laser power of 10 mW. In both cases (Fig. 5.7 (a, b)), a broadening of EPI spectral singularities in the signal being detected is visible.

With increasing irradiation power, at least up to ~15 mW, the video response amplitude was proportional to the power.

For temperatures below T_λ=2,17 K, no signal could be registered even for maximum laser power, in contrast to the experiments with direct irradiation of contact. The disappearance of the signal upon an improvement of heat removal due to a transition of Helium to its superfluid state confirms the hypothesis of the thermal nature of the observed effect.

Special experiments were carried out for estimating the heat constant τ of structure “substrate-film-spear”. For this purpose, the response signal was measured for a constant bias voltage V=17 mV across the NC in the static regime by using a compensation DC microvoltmeter and in the dynamic regime in

accordance with the above technique with a modulation frequency f=420 Hz for the radiation intensity. The signal amplitude was found to be exactly twice as high in the static regime. In view of the symmetry of the modulator, it can be concluded from such a result that the structure under consideration has a time constant τ<1/420 s~2,4·10^{-3} s.

The thermal origin of the response V_d measured by us is also confirmed by calculations carried out for the NC presented in Fig. 5.7 (b). Calculations were made by using the experimental values of the IVC, its first and second derivatives, obtained in absence of radiation. The absolute value of the response signals, V_d~10^{-6} V, is 2-3 orders of magnitude smaller than the error in the measurement of the IVC. Hence, more accurate values of the IVC were obtained by doubly integrating the values of the second derivatives. Experimental IVC were used for transforming the voltage dependences into current dependences. The IVC calculated in this way was found to coincide practically with the experimental IVC.

From a comparison of height and half-width of the T-peak in the PC spectra measured under laser irradiation with the PC spectra of Cu recorded in [16] at different temperatures we estimated the temperature increase ΔT to amount to 5 K. The obtained dependences correctly reflect the shape of the experimentally observed signal, although the absolute peak values are slightly higher (see line 1 in Fig. 5.7 (b) and Fig. 5.8). Moreover, calculations show that the amplitude of response signal has a non-linear dependence on temperature increase ΔT. The observed discrepancies with experiment are associated with

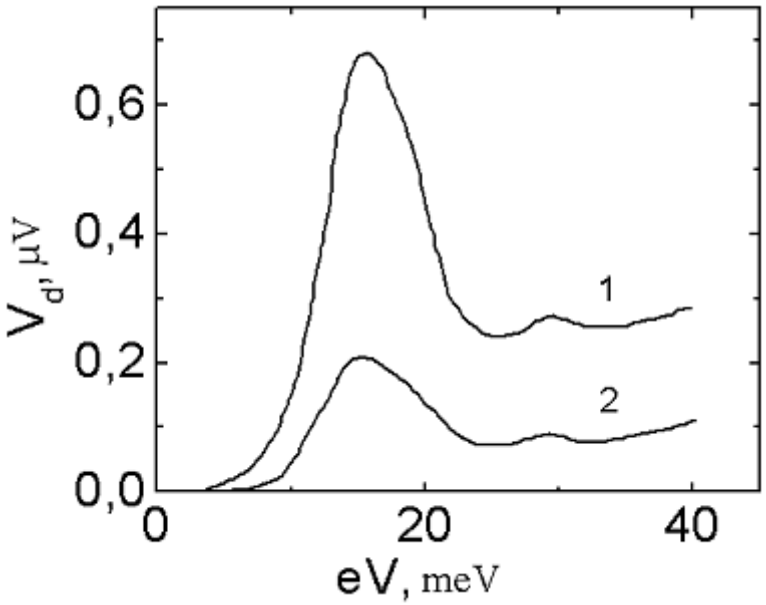

Fig. 5.8 Calculated values of point-contact signal for a temperature increase ΔT=10 K (1) and 5 K (2).

approximations used for simplifying the calculations, and with a nonsymmetric heating of electrodes in the NC region under actual experimental conditions.

So far, we have considered the results for small-size pure NCs with electrons moving in the ballistic regime. Such contacts have a resistance of 10-20 Ohm. For the contact whose PC spectrum is shown in Fig. 5.7 (b), the maximum intensity of spectrum gives a value g_{pc}^{max}~0,24, which is characteristic for the ballistic regime in a Cu contact [4]. An increase in geometrical size of the current concentration region leads to a change in electron-phonon kinetics, and a transition to the diffusive regime. Our measurements show that the shape of the response signal also undergoes a significant change for such contacts as illustrated in Fig. 5.9.

As can be seen in Fig. 5.9, the spectral components are

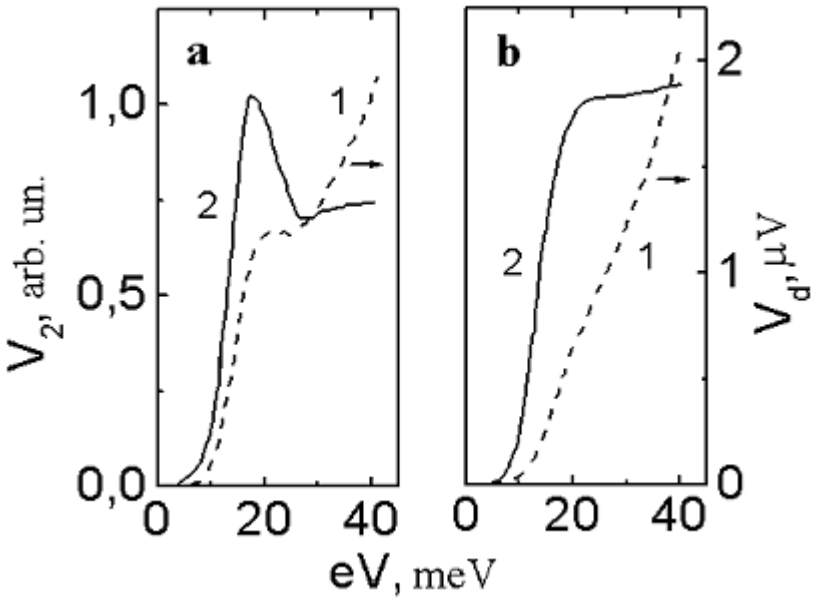

Fig. 5.9 Change in shape of the response signal for different types of Cu NCs: response signal obtained under optical irradiation on the back side of contact (1); point-contact spectrum of the same nanocontact (2).

smoothed upon transition to the thermal regime, and the response signal acquires a monotonic component that increases sharply with increasing of bias voltage. In these conditions, the measured signal cannot be associated only with a smoothing of EPI spectral singularities due to thermal broadening of the Fermi edge as a consequence of irradiation. This is so because the NC temperature in the thermal regime is given by the constant bias (see (2.16)) and is much higher than the quantity ΔT associated with laser heating.

5.4.2 Theoretical Basis of the Laser Thermal Point-Contact Spectroscopy

The entire body of experimental data makes it possible to formulate the basic concepts of a special type of PCS, - the Laser Thermal Point-Contact Spectroscopy. In the modulation temperature spectroscopy technique presented in [17], the change in contact temperature is due to the transport current, and the banks (bulk electrodes) remain cold due to a strong current spreading. Exposure of the NC to the optical laser radiation results in a heating of the electrodes in the immediate vicinity of the constriction, which is equivalent to an increase in the Helium bath temperature by an amount ΔT. The heating asymmetry due to irradiation of only one electrode (Fig. 5.6 (b)) should not affect the results significantly according to the data presented in Fig. 5.7. Apparently, the effect is felt more strongly on the amplitude of the signal being registered than on its shape.

The experimental signal V_d is the difference between two IVC of the NC at the temperatures T and $T+\Delta T$, respectively. To calculate this difference, we use the expression for the IVC of a metal NC from [18]:

$$I(V) = \frac{V}{R_0} - c\int_0^\infty \left[\frac{\varepsilon - eV}{e^{\beta(\varepsilon - eV)} - 1} - \frac{\varepsilon + eV}{e^{\beta(\varepsilon + eV)} - 1} + \frac{2eV}{e^{\beta\varepsilon} - 1} \right] g_{pc}(\varepsilon) d\varepsilon \tag{5.1}$$

where $\beta = (k_B T)^{-1}$, $c = 8d/3ev_F R_0$ and $g_{pc}(\varepsilon)$ - the NC EPI function.

For a small temperature increase ($\delta T << T$), the current response can be presented in the form $\delta I \sim (\partial I(V)/\partial T)\delta T$. Omitting terms in (5.1) that do not have a singularity at the point $\varepsilon = eV$ and

differentiating, we obtain the following expression for the inelastic component of the current:

$$\delta I(V) \cong -c\delta T \cdot T \int_0^\infty g_{pc}(\varepsilon)\chi_1\left(\frac{\varepsilon - eV}{k_B T_0}\right)d\varepsilon\,, \qquad (5.2)$$

where

$$\chi_1(y) = \frac{1}{k_B T}\left(\frac{y}{2sh\left(y/2\right)}\right)^2$$

is the thermal broadening function.

For a crystal where lattice vibrations are represented with the Einstein model ($g(\varepsilon)=g_0\delta(\varepsilon - \varepsilon_0)$), the emergence of a spectral singularity in response to laser irradiation is presented schematically in Fig. 5.10.

In the case of strong heating ($\Delta T>T_0$), we must compute the difference between two expressions (5.1). Assuming that the elastic component of the current does not change upon irradiation and that the temperature is low, we obtain an expression analogous to (5.2) but with a different thermal broadening function:

$$\chi_2(y) = \frac{1}{k_B \Delta T}\frac{|y|}{e^{|y|}-1}\,, \qquad y = \frac{\varepsilon - eV}{k_B \Delta T}\,. \qquad (5.3)$$

The peak half-width for the functions χ_1 and χ_2, is $6k_BT$ and $2{,}5k_BT$, respectively, and not $5{,}44k_BT$ as for conventional low frequency PCS.

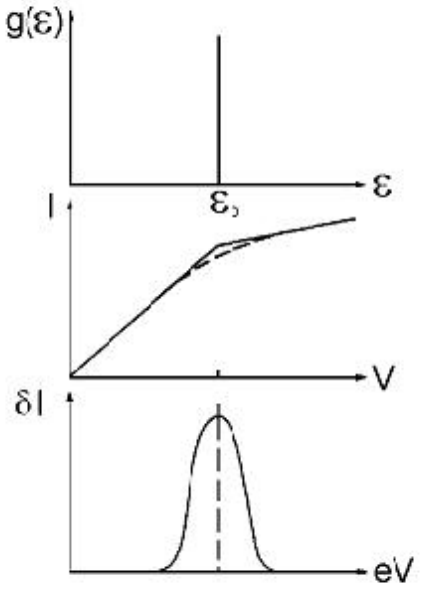

Fig. 5.10 Emergence of spectral singularity in laser response for the Einstein model of crystal lattice vibrations.

5.5 Characteristics of Ballistic Nanocontacts Exposed to Radiation from Acoustic to Optical Frequency Range

The results presented above show that the response of clean ballistic NCs when exposed to electromagnetic radiation can be determined by different mechanisms: the detection of a HF current or contact heating through irradiation in the optical range. To distinguish the frequency ranges for responses of different nature, we systematically studied the non-linear properties of ballistic NCs in the wide frequency range, similarly to what we did for the NCs in thermal regime and described in Chapter 4.

The results of these investigations [19] for the Cu NCs are presented in the remainder of this chapter.

The typical dependencies of the response signal on the bias $V_d(V)$ for different frequencies, shown in Fig. 5.11, are similar, as far as their common features are concerned, to the EPI spectrum of a clean Cu NC where electrons are moving ballistically.

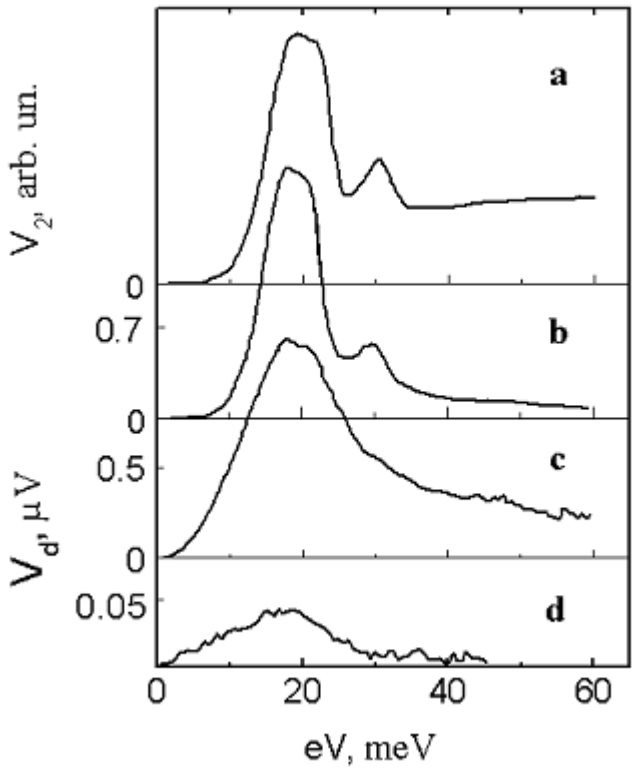

Fig. 5.11 Experimentally measured responses of a Cu nanocontact when exposited to radiation at frequencies $\Omega/2\pi$*: 3746 Hz (a);* $7{,}9\cdot10^{10}$ *Hz (b);* $2{,}5\cdot10^{12}$ *Hz (c);* $4{,}3\cdot10^{12}$ *Hz (d).*

In these measurements of the response when exposed to electromagnetic radiation in different frequency regions, the radiation was supplied to NCs by different methods: with the help of a waveguide in for wavelengths in the microvawe range, employing the light guide in the IR range, through the the windows in the lateral walls of the cryostat and lenses in the visible range. Hence the dependencies $V_d(V)$ presented in Fig. 5.11 refer to different NCs, the only exception being lines (a) and (b), which were obtained for the same NC. For the sake of further comparative analysis, Figs. 5.11 and 5.12 show the results for NCs with analogous PC spectra, similar to line (a) in Fig. 5.11.

The dependence of the response signal on bias voltage is determined by the relation between the frequency of the external field, Ω, and the characteristic relaxation time in the electron-phonon system. Comparing curves (a) and (b) in Fig. 5.11 (a) one can observe a decrease in background signal amplitude when exposing to an electromagnetic field with a frequency of $7{,}9\cdot10^{10}$ Hz. This decrease is associated with the process of reabsorption of non-equilibrium phonons, which determines the level of the background part of the signal in the PC spectrum. The reciprocal time of relaxation for these processes for Cu is equal to $5\cdot10^9$ Hz. This value is calculated from the frequency dependence of background reduction coefficient $\eta(f)$ (2.21), according to the method described in [20]. With this characteristic value we can attribute the dependences (a) and (b) in Fig. 5.11 to two limiting cases, namely line (a) to $\Omega\tau_{ph\text{-}e}<1$ and line (b) to $\Omega\tau_{ph\text{-}e}>1$.

The main part of the signal obtained for bias voltages $eV<30$ meV across NC is attributed to rectification of the alternating HF current at the IVC non-linearities associated with the emission of non-equilibrium phonons during the energy relaxation of electrons. For such processes, $\Omega\tau_{e\text{-}ph}<1$ (where $1/\tau_{e\text{-}ph}\sim10^{13}$-$10^{14}$ Hz) for all frequencies of the external field that were used to

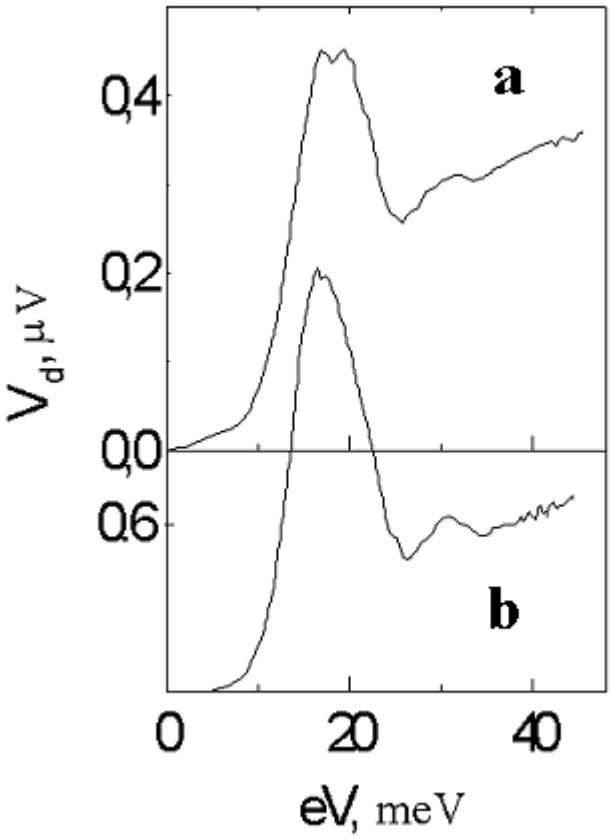

Fig. 5.12 Video response of a Cu contact for frequencies $\Omega/2\pi$*:* $2{,}8\cdot10^{13}$ *Hz (a) and* $4{,}75\cdot10^{14}$ *Hz (b).*

generate the curves presented in Fig. 5.11. The observed broadening of spectral singularities in the bias dependencies of the response with increasing frequency of irradiation, is associated with a transition from the classical to the quantum detection regime. This transition occurs when the quantum energy of the external field (f~$2{,}5\cdot10^{12}$ Hz) becomes comparable to the width of the energy region of a non-linear singularity on the IVC (~10 meV for Cu) of the NC. The decrease in signal

amplitude (Fig. 5.11) with increasing irradiation frequency is naturally associated with a deterioration of the antenna properties of the wire electrode of the NC: decreasing the wave length of the incident radiation, the amplitude of the alternating HF current induced in the NC decreases correspondingly.

Upon a further increase in frequency, the form of bias dependence of $V_d(V)$ changes radically. Fig. 5.12 shows the results obtained for exposure to radiation with frequencies $2{,}8\cdot10^{13}$ Hz and $4{,}75\cdot10^{14}$ Hz. In this range, $\Omega\tau_{e\text{-}ph}\sim1$, and hence we can expect an even stronger broadening of EPI spectrum compared to Fig. 5.11. However, Fig. 5.12 shows that the EPI spectrum as a function of the response becomes still sharper, especially in the visible range. We have shown earlier (section 5.4) that the response of metal NCs to optical radiation is of different nature and associated with thermal broadening of the Fermi edge in the energy distribution of electrons. The results presented in Figs. 5.11 and 5.12 lead to the conclusion that a change in response mechanism from rectification to heating of the NC by external radiation occurs in the frequency range $4{,}3\cdot10^{12}$ - $2{,}8\cdot10^{13}$ Hz.

To analyze the behaviour of a metal NC in a HF electromagnetic field, we use the expression for the IVC obtained in [18] that considers also reabsorption of non-equilibrium phonons,

$$I(V)=\frac{V}{R_0}-C\int_0^{\infty}\left[\frac{\omega-eV}{e^{\beta(\omega-eV)}-1}-\frac{\omega+eV}{e^{\beta(\omega+eV)}+1}+2eVN(\omega)\right]g_{pc}(\omega)d\omega \tag{5.4}$$

where $C=8d/3e\hbar v_F R_0$; $\beta=1/k_BT$; and $N(\omega)$ - the energy distribution function for non-equilibrium phonons for the case of their full reabsorption:

$$N(\omega)=\frac{1}{4\omega}\left[\frac{2\omega}{e^{\beta\omega}-1}+\frac{\omega-eV}{e^{\beta(\omega-eV)}-1}+\frac{\omega+eV}{e^{\beta(\omega+eV)}-1}\right] \tag{5.5}$$

where R_0 is contact resistance at V=0.

With these formulae we can calculate the IVC and the bias voltage dependence of second IVC derivative, d^2I/dV^2 for a Cu NC with resistance R_0=5 Ohm. The NC diameter was determined from (2.2) for a clean orifice, and the value of the Cu EPI function taken from data tabulated in [4] was used for $g_{pc}(\varepsilon)$. The obtained dependence is shown in Fig. 5.13 and agrees well with the real PC spectrum of a Cu NC measured experimentally at acoustic frequency 3746 Hz (Fig. 5.11 (a)).

Line 2 in Fig. 5.13 shows the bias dependence of the effective temperature $T^*(V)$ of non-equilibrium phonons with distribution $N(\omega)$. The effective temperature was determined from the condition that the energy supplied to electron subsystem by the non-equilibrium phonon system, has to be balanced by the energy distribution of equilibrium phonons with the temperature T^*:

$$\int_0^\infty \frac{\varepsilon g_{pc}(\varepsilon)d\varepsilon}{e^{\varepsilon/k_BT^*}-1}=\int_0^{eV}\omega g_{pc}(\omega)N(\omega)d\omega \tag{5.6}$$

The dashed line in Fig. 5.13 shows the simplified dependence $T^*(V)=eV/4k_B$, which was also proposed in [18] for a case of complete reabsorption of non-equilibrium phonons.

The good correspondence of calculated and experimentally measured PC spectra gives the possibility to apply the described above procedure for calculations of the NC response when

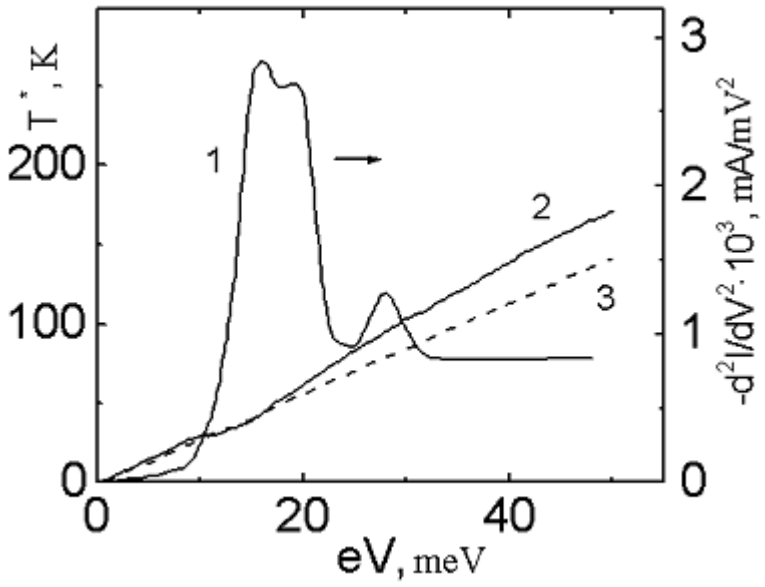

Fig 5.13 Theoretical spectrum of a Cu nanocontact (1) and the dependence of effective temperature of non-equilibrium phonons (2, 3) on bias voltage across the nanocontact, according to different models.

exposed to HF radiation.

Calculations were made without taking into account the changes in coupling between the NC and the external field at different wavelengths, and the alternating HF voltage induced in the NC was assumed to be equal to V_1=1 mV at all frequencies. The obtained dependences $V_d(V)$ for the three electromagnetic fields where $\hbar\Omega$= 0,3 meV, 10,6 meV and 17,6 meV, presented in Fig. 5.14 (a), correspond well to the form of experimental lines in Fig. 5.11. The fitting parameter used in these calculations is the amplitude of the HF voltage on the contact V_1. With the values 0,30 mV; 0,55 mV and 0,19 mV for the frequencies

$7{,}9\cdot10^{10}$ Hz, $2{,}5\cdot10^{12}$ Hz and $4{,}3\cdot10^{12}$ Hz correspondently, we obtained good quantitative agreement with experimental data.

A consideration of non-equilibrium phonons in the NC leads to a nonzero response at high voltages in the calculation, in contrast to [21], where non-equilibrium phonons were neglected.

In the optical frequency range, the response mechanism is of thermal nature. Hence we calculated the differences between the IVC of contacts according to (5.4) and (5.5) for various values of the temperature increase ΔT caused by laser irradiation:

$$V_d(V) = \left[I(V,T) - I(V,T_0)\right]\frac{dV}{dI}(V), \qquad (5.7)$$

where the temperature increase in the NC is $\Delta T = T - T_0$ and the temperature of the Helium bath T_0=2,8K.

The theoretical lines presented in Fig. 5.14 (b) correctly describe the main features of the experimentally obtained dependences shown in Fig. 5.12. The maximum value of the response signal for line 3 in Fig. 5.14 (b) is 7,38 μV.

By absorbing laser radiation in the optical range ($\Omega/2\pi$=$4{,}75\cdot10^{14}$ Hz), the conduction electrons in the metal acquire an excess energy $\hbar\Omega$~2 eV, which is about 70 times higher than the energy of Debye phonons in copper ($\hbar\omega_D$~28 meV). As a result of the subsequent cascades of relaxation processes in the electron-phonon system, a steady non-equilibrium state is established. The extent of deviation of electron and phonon subsystems from equilibrium is determined by the intensity of the laser pumping, as well as by the characteristic velocities of uniform and non-uniform relaxation of

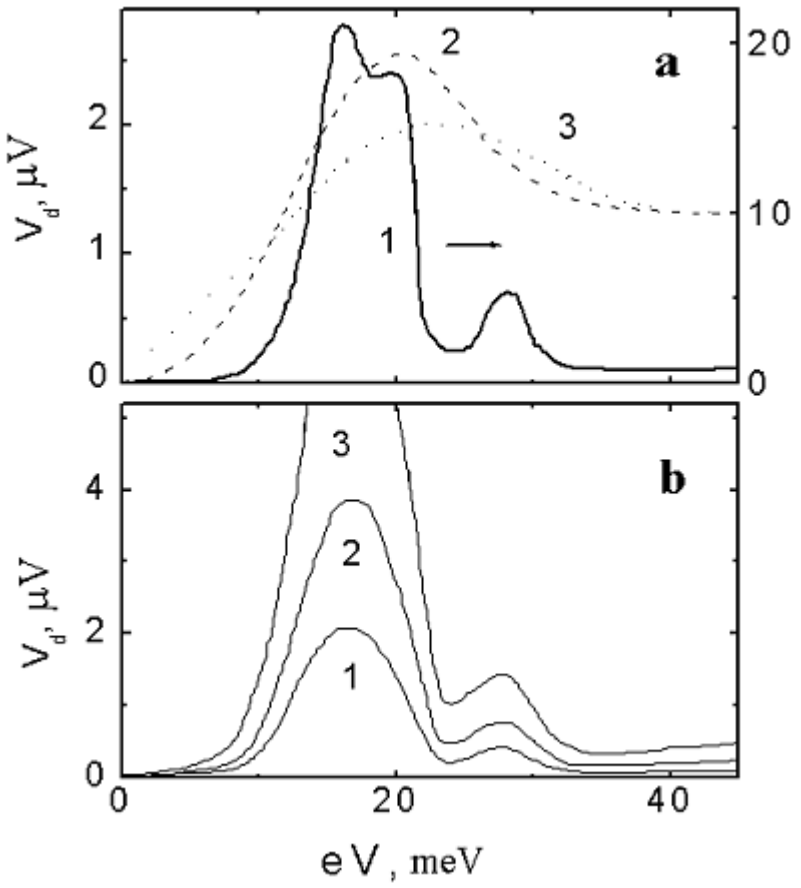

Fig. 5.14 (a) - Response signal calculated for three radiation frequencies Ω/2π: 7,9·10[10] Hz (1), 2,5·10[12] Hz (2) and 4,3·10[12] Hz (3). (b) - Dependences of differences between I-V characteristics on bias for a temperature increase, ΔT, amounting to 1,8 K (1), 2,8 K (2) and 4,1 K (3).

quasiparticles. To simplify calculations, we assumed that in the optical spectral region, the role of radiation is reduced just to a steady heating of NC. The equilibrium energy distribution function is chosen for phonons with a higher value of temperature than that of Helium bath.

A comparison of Figs. 5.12 and 5.14 (b) shows that the calculated response signal is in general (even quantitative) agreement with the experimental results. An exception to this is the high bias region, where there is almost monotonous growth of the measured response amplitude, as for the dirty NC (section 4.3).

An estimate of the NC overheating by laser radiation from the broadening of the low-energy peak of the PC spectrum measured in [14] gives a value of about 1K for ΔT. For a constant intensity of radiation, this quantity may vary slightly in different experiments due to differences in the tuning of laser radiation to the contact region.

Measurements made by us using a CO_2 laser ($\hbar\Omega$=117 meV) gave a response pattern similar to that for the He-Ne laser (see line 1, Fig. 5.14 (b)).

Thus, our experimental results lead to the conclusion that starting from frequencies ~$2{,}8\cdot10^{13}$ Hz, the bolometric response begins to dominate over the signal associated with the rectification of the HF current induced in the NC by an external field.

It should be noted that there is no guarantee that the NC is directly under the laser spot since the contact size (d~10 nm) is much smaller than the diameter of the copper pin (D~1 μm).

Let us now consider in detail the possible reasons why laser heating causes a contribution to the response of a metal NC to emerge, which depends linearly on bias voltage. Fig. 5.15 shows the PC spectrum of a copper contact (a) having a resistance R_0=14,7 Ohm and a dependence of the response to optical radiation (b) for two values of the He-Ne laser power. The expressions for the absolute values of the intensity of PC spectra

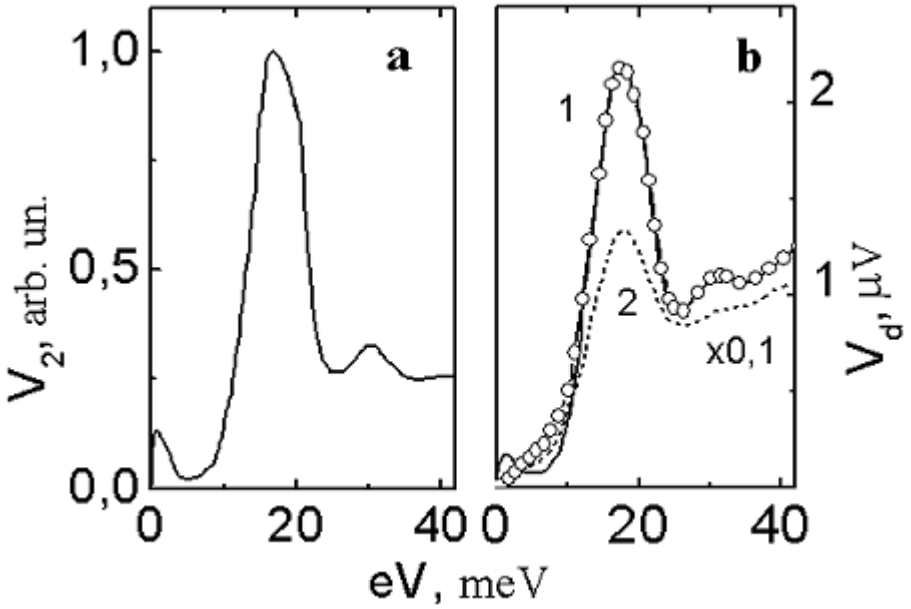

Fig. 5.15 Spectrum of a Cu nanocontact in the ballistic regime (a) and its response to optical radiation (b) for a laser power of 3,8 mW (1) and 25 mW (2). The solid lines correspond to experimental results while the points indicate the results of calculations. The vertical scale for the line (2) is reduced 10 times.

for copper and the contact resistance (Wexler's equation (2.3)) were used to calculate the elastic mean free path of electrons and the contact diameter (l_i=1300 nm, d=7,8 nm). Since $l_i/d>>1$, the contact is clean and the electrons follow the ballistic regime. This conclusion is also confirmed by the good quality of the spectrum in Fig. 5.15 (a).

In analogy with the response of a dirty contact (Chapter 4) to optical radiation, we assume that clean contacts also make a linear bolometric contribution to the signal being measured:

$$V_d^b(V) = I\frac{dR}{dT}\Delta T = V\alpha_T\Delta T \qquad (5.8)$$

where V is the voltage, ΔT the increase in temperature as a result of irradiation, and $\alpha_T=R_0^{-1}\cdot(dR/dT)$ the thermal coefficient of the metal resistance in the NC region. In the case of a complete reabsorption of non-equilibrium phonons for large bias voltages across the contact (phonon signal region), there exists a simple relation between α_T and the background level $\alpha_V=R_0^{-1}\cdot(dR/dV)$ in the low-frequency PC spectrum. The relation α_T/α_V determines the level of phonon overheating in the NC. For clean contacts, we obtain the theoretical estimation α_T/α_V =0,172 mV/K [20]. Using this value, α_V=3,85·10^{-3} mV^{-1} calculated from the experimental line in Fig. 5.15 (a) for V>35 mV, and putting ΔT=2 K, we obtain V_d^b=66 μV for V=50 mV, which is about two orders of magnitude higher than the experimental values presented by line 1, Fig. 5.15 (b).

If we assume only a partial reabsorption of non-equilibrium phonons by the electron flow, as is usually the case with clean contacts of small geometrical dimensions, the relation between the phonon gas temperature T^* and the voltage will be weaker than that shown in Fig. 5.13 (line 2). In this case, the experimental value [21] of the ratio α_T/α_V is about twice as large as the theoretical value. Hence the response signal also must increase by a factor of two.

It is more reasonable to assume that the linear bolometric contribution to the NC response $V_d^b(V)$ is associated not with the contact itself, but with the region surrounding it, *i.e.* the volume of the bulk electrodes around the contact (~0,1 mm) over which the transport current spreads. The voltage drop in this region is much smaller than the one across the NC, and the value of α_T is also different. Both these quantities are position depended. Hence

an exact calculation of $V_d^b(V)$ requires a solution of the spatially non-uniform relaxation problem.

Under actual conditions, the experimental measurements of the response of a NC to laser heating are carried out by registering the sum of the signals $V_d(V)=V_d^b(V)+V_d^T(V)$, where $V_d^T(V)$ is defined by formula (5.7) and $V_d^b(V)$ by expression (5.8). We calculated the dependence $V_d(V)$ for the case ΔT=2 K by introducing a fitting parameter A=1,73·10^{-5} K^{-1} ($V_d^b(V)=A\cdot\Delta T\cdot V$) which takes into account the change in voltage as well as the thermal resistance coefficient in the vicinity of the contact. The results of such calculations are marked by circles in Fig. 5.15 (b) and are in good agreement with the experimental data.

To interpret the experimental results, we should apparently take into account the possible steady deviation from the equilibrium values of the distribution functions for electrons and phonons under the action of laser radiation with a high energy $\hbar\Omega>>\hbar\omega_D$, instead of reducing the effect of irradiation just to heating of the contact.

Without laying any claim to the rigorous nature of the model chosen by us, we calculated the difference $V_d(V)$ between two IVC of a copper NC described by expression (5.4). The action of the laser radiation for the perturbed IVC was taken into consideration not only by replacing T_0 by $T_0+\Delta T$, but also by adding to the non-equilibrium phonon distribution function (5.5) a term

$$M(\varepsilon)=\gamma(B-\varepsilon)\frac{\Theta(B-\varepsilon)}{\varepsilon}. \qquad (5.9)$$

The results of calculations for the values B=30 meV and $\gamma\sim10^{-4}$ were found to be practically the same as for the dependence shown by circles in Fig. 5.15 (b). Although the function $M(\varepsilon)$ is close to the phonon equilibrium distribution function, its value

becomes much larger at high energies for the chosen values of parameters. The final conclusion about the possible extent of the deviation from equilibrium in the electron-phonon system in a NC exposed to laser radiation can be drawn after carrying out a more rigorous theoretical analysis.

5.6 Conclusions

The response V_d to irradiation in the HF range is found to be not only due to rectification of the HF current, but also to a bolometric effect which modifies the IVC. For contacts in the ballistic regime this effect is attributed to an increase in the effective temperature of the phonon subsystem, while the electron subsystem continues to be at ambient temperature. At the high enough frequencies $f>f_{ph\text{-}e}$ ($f_{ph\text{-}e}$ is phonon-electron relaxation frequency), at small bias ($eV<hf_D$) the response signal is determined mainly by the rectified HF current. With increasing bias, this part tends to zero, while the bolometric part, proportional to the first derivative of the IVC, grows.

Improved resolution of PCS at frequencies $f>f_T, f_{ph\text{-}e}$, due to the reduced reabsorption of non-equilibrium phonons was established and allowed to consider the High Frequency Point-Contact Spectroscopy as a new type of PCS.

The non-equilibrium Debye phonons relaxation on electrons occurs at the inter-atomic scale, while the NC dimension is about 10-100 inter-atomic distances. Thus, the value for relaxation frequency of such a process for copper, $f_{ph\text{-}e}=5\cdot10^9$ Hz, experimentally obtained by us from High Frequency Point-Contact Spectroscopy studies, is valid for bulk copper.

A significant increase in the background part as a function of bias was observed for normal and inverse ($d^2V/dI^2<0$) spectra for Sb. The registered weak frequency dispersion of the background in the Sb PC spectra points towards a low intensity of

reabsorption processes of non-equilibrium phonons. This means the latter can leave the NC region without being scattered by electrons. Observed high level of residual background for f~80 GHz can't be attributed to the bolometric effect. In all probability, the residual background is due to rapid electron-phonon scattering processes with a high characteristic frequency $f_{e\text{-}ph} \sim \lambda f_D \sim 10^{13}$ Hz.

Copper NCs were investigated under irradiation in a wide frequency range, from acoustic to optical frequencies (10^3-$4{,}78 \cdot 10^{14}$ Hz). The main part of the response signal obtained for frequencies up to ~$4{,}3 \cdot 10^{12}$ Hz at, low bias voltages (eV<30 meV) is attributed to classical rectification of the alternating HF current at the non-linearities in the IVC, associated with the emission of non-equilibrium phonons during energy relaxation of the electrons. The observed broadening of spectral singularities at frequencies above f=$2{,}5 \cdot 10^{12}$ Hz is associated with a transition from classical to quantum detection. For f>$2{,}8 \cdot 10^{13}$ Hz the response signal is attributed to the bolometric effect.

Exposure of the NC to the optical laser radiation (λ=0,63 μm) results in a heating of the electrodes in the immediate vicinity of the constriction, which is equivalent to an increase in the Helium bath temperature. The entire body of experimental data makes it possible to formulate the basic concepts of a special type of Point-Contact Spectroscopy for the optical range of frequency, - the Laser Thermal Point-Contact Spectroscopy. The mechanism for the video response of the NC for low bias voltages (eV<hf_D) under optical radiation is attributed to the heating of the NC by laser radiation since heating broadens the Fermi edge.

We obtained a good agreement between experimental data and theoretical calculations, except for the response to radiation in the optical range obtained for high bias voltages (eV>hf_D). In analogy with the response to optical radiation of NCs in the thermal regime, we assume that the bolometric contribution is associated

not with the NC itself, but with its surrounding region, *i.e.* with the volume of bulk electrodes (~0,1 mm) around NC, over which the transport current spreads.

References

1. I. K. Yanson, O. P. Balkashin, Yu. A. Pilipenko. Non-equilibrium phonon relaxation in metal microcontacts. Sov. Phys. JETP Lett. vol. 41, No. 7, p. 373 (1985)

2. O. P. Balkashin, I. K. Yanson, Yu. A. Pilipenko. Relaxation kinetics of non-equilibrium phonons in copper and gold. Sov. J. Low Temp. Phys. 13, 222 (1987)

3. A. G. M. Jansen, A. P. van Gelder, P. Wyder. Point–contact spectroscopy in metals. J. Phys. C, 1980, v.13, N 33, p.6073-6118

4. A. V. Khotkevich and I. K. Yanson. Atlas of Point Contact Spectra of Electron-Phonon Interaction in Metals. Kluver Academic Publishers, Boston/Dordrecht/London (1995)

5. O. P. Balkashin, I. I. Kulik. Laser thermal point-contact spectroscopy of metals. Sov. J. Low Temp. Phys. 16 (1990), pp. 166–171

6. I. K. Yanson, O. I. Shklyarevskii, N. N. Gribov. Anisotropy of electron-phonon interaction spectra in a magnetic field and quantum interference effects in antimony point contacts. Sov. J. Low Temp. Phys., 1992, v.88, N 1/2, pp. 135-162

7. I. K. Yanson, N. N. Gribov, O. I. Shklyarevskii. Trajectory effects in microcontact spectroscopy of the electron-phonon interaction. JETP Lett. 42, 195 (1985)

8. O. P. Balkashin, I. I. Kulik. Relaxation kinetics for non-equilibrium quasi-particle excitations in antimony point contacts. Sov. J. Low Temp. Phys. 21 (1995), pp. 32-37

9. O. P. Balkashin, I. I. Kulik. Quasi-particle relaxation kinetic in Sb point contacts. Proc. 2nd International Conference Of The Point Contact Spectroscopy. Physica B 218 (1996) 50-53

10. I. F. Itskovich, I. O. Kulik, R. I. Shekhter. Effect of Localization and Inelastic Scattering of Electrons in Point-Contact Electric Conductivity. Sov. J. Low Temp. Phys. 13, 659 (1987)

11. I. O. Kulik, M. V. Moskalets. Nonlinear electrical conductivity of metal point contacts in the dirty limit. Sov. J. Low Temp. Phys. 15, 229 (1989)

12. G. Bergmann, W. Wei, Z. Yao, R.M. Mueller. Non-equilibrium in metallic structures in the presence of high current density. Phys. Rev. B, 1990, v.41, n 11, p. 7386-7396

13. J. Liu, N. Giordano. Weak localization, electron-electron interactions and Joule heating in the presence of a microwave electric field in thin metal films. Phys. Rev. B, 1991, v.43, n 2, p. 1385-1390

14. O. P. Balkashin, I. I. Kulik. The interaction of laser radiation with copper microcontacts. Proc. Young Scientist's Conference, Kharkov, 1989, pp. 96-97. Institute for Low Temperature Physics & Engineering Ukr. SSR Acad. Sci. (in Russian)

15. I. O. Kulik, A. N. Omel'yanchuk, I. G. Tuluzov. Motional inductance of the point-contacts between normal metals. Sov. J. Low Temp. Phys, 8, 386 (1982)

16. A. P. van Gelder, A.G.M. Jansen, and P. Wyder, Temperature dependence of point-contact spectroscopy in copper. Phys. Rev. B, 1980, v.22, n 4, p. 1515-1521

17. B. I. Verkin, I. K. Yanson, I. O. Kulik, O. I. Shklyarevskii, A. A. Lysykh, Yu. G. Naidyuk.. Singularities in d^2V/dI^2 dependences of point contacts between ferromagnetic metals. Solid State Commun. 30, 215 (1979)

18. I. O. Kulik. Non-equilibrium current states in the metal micro-contacts. Sov. J. Low Temp. Phys. 11, 516 (1985).

19. O. P. Balkashin, I. I. Kulik. The characteristics of the metal point contacts (PC) in the range between acoustic and optical frequencies. Sov. J. Low Temp. Phys. 18 (1992), pp. 946–952

20. I. O. Kulik, I. K. Yanson, O. P. Balkashin, Yu. A. Pilipenko, I. I. Kulik. A method for the determination of the relaxation time for non-equilibrium excitations. USSR Patent No. 1581138, March 22, 1990

21. I. O. Kulik, A. N. Omel'yanchuk, I. G. Tuluzov, T. Z. Sarkisyants. Effects of high frequency detection in microcontacts between normal metals. Sov. J. Low Temp. Phys. 10 (1984), p. 463

22. I. O. Kulik, A. N. Omel'yanchuk, I. K. Yanson. Non-equilibrium phonons in the point-contacts between the normal metals. Sov. J. Low Temp. Phys. 7, 129 (1991)

23. A. I. Akimenko, A. B. Verkin, N. M. Ponomarenko, I. K. Yanson. Dependence of point-contact spectra on contact parameters. Sov. J. Low Temp. Phys. 8 (1982), p. 130